Title

m6A-modification of cyclin D1 and c-myc IRESs in glioblastoma controls ITAF activity and resistance to mTOR inhibition

Authors

Benavides-Serrato, Angelica
Saunders, Jacquelyn T
Kumar, Sunil
et al.

Publication Date

2023-05-01

DOI

10.1016/j.canlet.2023.216178

Peer reviewed

HHS Public Access

Author manuscript

Cancer Lett. Author manuscript; available in PMC 2024 January 23.

Published in final edited form as:

Cancer Lett. 2023 May 28; 562: 216178. doi:10.1016/j.canlet.2023.216178.

m^{6}A-modification of cyclin D1 and c-myc IRESs in glioblastoma controls ITAF activity and resistance to mTOR inhibition

Angelica Benavides-Serrato[1,5], **Jacquelyn T. Saunders**[5], **Sunil Kumar**[5], **Brent Holmes**[5], **Kennedy E. Benavides**[5], **Muhammad T. Bashir**[1,5], **Robert N. Nishimura**[2,5], **Joseph Gera**[1,3,4,5]

[1]Department of Medicine, David Geffen School of Medicine at UCLA,

[2]Department of Neurology, David Geffen School of Medicine at UCLA,

[3]Jonnson Comprehensive Cancer Center, University of California-Los Angeles, California

[4]Molecular Biology Institute, University of California-Los Angeles, California

[5]Department of Research & Development, Greater Los Angeles Veterans Affairs Healthcare System, Los Angeles, California

Abstract

A major mechanism conferring resistance to mTOR inhibitors is activation of a salvage pathway stimulating internal ribosome entry site (IRES)-mediated mRNA translation, driving the synthesis of proteins promoting resistance of glioblastoma (GBM). Previously, we found this pathway is stimulated by the requisite IRES-*trans*-acting factor (ITAF) hnRNP A1, which itself is subject to phosphorylation and methylation events regulating cyclin D1 and c-myc IRES activity. Here we describe the requirement for m^{6}A-modification of IRES RNAs for efficient translation and resistance to mTOR inhibition. DRACH-motifs within these IRES RNAs upon m^{6}A modification resulted in enhanced IRES activity via increased hnRNP A1-binding following mTOR inhibitor exposure. Inhibitor exposure stimulated the expression of m^{6}A-methylosome components resulting in increased activity in GBM. Silencing of METTL3–14 complexes reduced IRES activity upon inhibitor exposure and sensitized resistant GBM lines. YTHDF3 associates with m^{6}A-modified cyclin D1 or c-myc IRESs, regulating IRES activity, and mTOR inhibitor sensitivity *in vitro* and in xenograft experiments. YTHDF3 interacted directly with hnRNP A1 and together stimulated hnRNP A1-dependent nucleic acid strand annealing activity. These data demonstrate that m^{6}A-methylation of IRES RNAs regulate GBM responses to this class of inhibitors.

Keywords

glioblastoma; drug resistance; mTOR inhibitors; N^6-methyladenosine modification; IRES; ITAF

Corresponding Author: Joseph Gera, Ph.D., Greater Los Angeles VA Healthcare System, 16111 Plummer Street (151), Building 1, Room C111A, Los Angeles, CA 91343. Phone: (818) 895-9416; Fax: (818) 895-9554; jgera@mednet.ucla.edu.

Appendix A. Supplementary data

Supplementary data for this article are available at *Cancer Letters* Online (http://www.sciencedirect.com/journal/cancer-letters)

1. Introduction

The median survival of patients with glioblastoma (GBM) has remained at a dismal twelve months, for one of the most prevalent and lethal of all central nervous system tumors [1–3]. The lethality of this neoplasm is due to the difficulties associated with complete surgical resection and the development of drug resistance [4]. The mutational landscape of glioblastomas includes expression of constitutively active variants and amplification of EGFR, as well as, PTEN loss and hyperactivation of the phosphatidylinositol 3-kinase (PI3K) cascade [1, 5, 6]. These mutations are observed in approximately seventy percent of GBMs and result in downstream hyperactivation of the mTOR kinase [7]. mTOR exists in at least two major complexes, mTOR complex 1 and 2 (mTORC1 and 2) and each kinase complex contains distinct regulatory subunits guiding substrate specificities [8]. The mTOR kinase complexes regulate protein synthesis, autophagy and metabolism thereby governing tumor cell growth, drug resistance and survival [9].

First generation allosteric mTOR inhibitors have failed in the clinic for GBM [10]. The limited efficacy of rapamycin and rapalogs has been demonstrated to be the result of incomplete mTORC1 blockade, the inability to inhibit mTORC2, and the loss of mTORC1 driven feedback regulatory mechanisms resulting in elevated AKT activity [11–14]. Second generation mTORC kinase inhibitors targeting both mTORC1 and 2 have also demonstrated limited benefits in clinical trials thusfar, as tumors have been shown to acquire resistance due to mutations in mTOR itself or activating mechanisms which bypass mTOR and induce cell proliferation [15, 16]. Thus, a complete understanding of the mechanisms leading to mTOR resistance in glioblastoma is required prior to the rational design of mTOR targeting therapies.

The complex signaling relationships between the mTORCs and the crosstalk mechanisms which have been described between the mTOR cascade and other major signaling pathways, suggest that many mechanisms of mTOR inhibitor resistance exist [4]. Our studies have demonstrated that both allosteric and direct mTOR kinase inhibitors are able to activate a transcript-specific protein synthesis salvage pathway capable of maintaining the mRNA translation of critical cell cycle determinants resulting in resistance to mTOR therapies [16]. Transcript-specific enhancement of translation upon activation of the salvage pathway is mediated via IRES-dependent protein synthesis and requires the ITAF, hnRNP A1 [17]. Recently, we have also described the identification of a small molecule inhibitor of hnRNP A1 which blocks cyclin D1 and c-myc IRES activity and synergizes with mTOR inhibitors to achieve strong anti-GBM activities [16, 18].

While previously we have shown that specific post-translational symmetrical di-methylation of arginine residues on hnRNPA1 are critical for its ITAF activity [19], in this report we describe m^6A-modifications required within the cyclin D1 and c-myc IRES RNAs for efficient IRES-mediated translation in the face of mTOR inhibition. We identified and characterized DRACH-motifs within these IRESs which were shown to enhance hnRNP A1-dependent ITAF activity following mTOR blockade. We demonstrate that in response to mTOR inhibition GBM cells stimulate m^6A-methylosome component expression and activity. Knockdown of METTL3–14 complexes ablated mTOR inhibitor induced IRES

activity and sensitized resistant GBM cells. YTHDF3 was found to bind to m^{6}A-modified IRES RNAs and regulate IRES activity and protein synthesis dictating mTOR inhibitor sensitivity both *in vitro* and in GBM xenografts. Additionally, we show that YTHDF3 is a protein partner of hnRNP A1 and cooperatively stimulate nucleic acid strand annealing.

2. Materials and Methods

2.1. Cell Lines, Transfections and Viral Transductions

All GBM cell lines were obtained from ATCC. HEK293 cells were kindly provided by Norimoto Yanagawa (Department of Medicine, UCLA). The patient-derived HK296 line was generously provided by Dr. Harley Kornblum (Department of Molecular & Medical Pharmacology, UCLA). Lines were routinely tested to confirm the absence of mycoplasma and authenticated by STR profiling (ATCC). DNA transfections were performed using Effectene transfection reagent according to the manufacturer (Qiagen, Germantown, MD). For siRNA knockdowns, lines were transfected with 10 nmol/L siRNA pools targeting human hnRNP A1, METTL3–14, YTHDF3 or a non-targeting scrambled control sequence. ON-TARGETplus siRNAs were obtained from Horizon Discovery Biosciences and transfected using Lipofectamine RNAimax (ThermoFisher Scientific). Viral transduction of the dominant-negative hnRNP A1 mutant and YTHDF3 constructs was performed as previously described [20].

2.2. Constructs and Reagents

The cyclin D1 and c-myc IRES mRNA reporter constructs have been previously described [21]. The LXSP-NLS-A1-A1 construct expressing the dominant negative hnRNP A1 shuttling mutant was a kind gift from Dr. Danilo Perrotti (Department of Biochemistry and Molecular Biology, University of Maryland). Site-specific m^{6}A mutagenesis was performed using the QuikChange Lightning Multi Site-Directed Mutagenesis Kit (Agilent Technologies) with the appropriate mutagenic primers to generate c-myc and cyclin D1 IRES luciferase reporter constructs. shRNA constructs (psi-LVRH1P) targeting human YTHDF3 and a scrambled sequence control were obtained from GeneCopoeia (#HSH069323). Recombinant YTHDF3 and hnRNP A1 was expressed and purified from HEK293 cells using anti-glutathione-Sepharose column chromatography as described previously [20]. Antibodies to the following proteins were used: mouse IgG (#sc-2025, Santa Cruz Biotechnology), hnRNP A1 (#ab5832, Abcam), anti-m^{6}A (#E1610, NEB), anti-HA (#ab9110, Abcam), METTL3 (#96391S, CST), METTL14 (#51104S, CST), METTL3–14 complex (#29313, Cayman), WTAP (#56501S, CST), FTO (#45980S, CST), ALKBH5 (#703570, ThermoFisher), YTHDF1 (#17479–1-AP, Proteintech), YTHDF2 (#ABE542, Millipore Sigma), YTHDF3 (#25537–1-AP, Proteintech), YTHDC1 (#A305–096A, Bethyl Laboratories), YTHDC2 (#35440S, CST), cyclin D1 (#2922, CST), c-myc (#9402, CST), and actin (#AM4302, ThermoFisher). PP242 and rapamycin were obtained from LC Laboratories (Woburn, MA). All other reagents were from Sigma-Aldrich.

2.3. Luciferase Reporter Assays, Proliferation Assays and Measurement of m^{6}A Methylation in Cells

The indicated reporter constructs (200 ng DNA) were transiently transfected into cells. Subsequently, cells were exposed to the indicated concentrations of PP242 for 24 h after which extracts prepared and luciferase activity determined as previously described [21]. Luminescence was measured using the Dual-Luciferase Reporter Assay System (Promega). Cell proliferation was determined using resazurin, XTT, or ^{3}H-thymidine uptake assays as described [19]. To measure the levels of m^{6}A methylation in cells (me-RIP), 1 μg of anti-m^{6}A antibody, 20 μg of fragmented cellular RNA and 20 μl of protein-G sepharose were incubated in buffer containing 100 nM NaCl, 0.1% NP-40, 10 mM Tris-HCl (pH7.4), 1 U/μl RNasin in 200 μl at 4°C for 2 h. Beads were subsequently washed and RNA isolated and utilized in qRT-PCR analyses.

2.4. *In Vitro* RNA-Pull Down, Quantitative RT-PCR, Filter Binding Assays, and Polysome Analysis

RNA-pull down assays were performed as previously described [20]. Briefly, cytoplasmic lysates were prepared and cleared via centrifugation. 10 μg of *in vitro* transcribed biotinylated RNA was added to the supernatant and incubated for 1 h at 4°C. Protein and biotinylated RNA complexes were recovered by the addition of 30 μl of streptavidin-Sepharose and subsequently washed and subjected to immunoblot analyses. For quantitative RT-PCR, extraction of RNA was performed using Trizol® reagent (ThermoFisher Scientific). Total RNA was then quantified and integrity assessed using an Agilent 2100 Bioanalyzer (Agilent Technology). Total RNA was reverse transcribed with random primers using the iScript™ cDNA synthesis kit from Bio-Rad. SYBR® Green quantitative PCR (MilliporeSigma) was performed in triplicate in 96-well optical plates on an ABI Prism 7000 Sequence Detection System (ThermoFisher Scientific) according to the manufacturer's instructions. Primer sequences are available upon request. For filter binding assays, the indicated amounts of GST-tagged hnRNP A1 was added to *in vitro* transcribed ^{32}P-labeled RNAs corresponding to either native or those containing a site-specific adenosine methylation on either cyclin D1 or c-myc sequences. Binding reactions were performed in a volume of 10 μl in buffer containing 5 mM HEPES (pH 7.6), 30 mM KCl, 2 mM $MgCl_2$, 200 mM DTT, 4% glycerol and 10 ng yeast tRNA for 10 min at room temperature [18, 20]. 8 μl of each reaction was applied to nitrocellulose membranes, washed, dried, and signals quantified using a PhosphorImager. Binding curves were fitted by using SigmaPlot to determine the apparent dissociation constants. Polysome analysis was performed as previously described [20]. Briefly, cells were lysed in buffer containing 100 μg/ml of cycloheximide at 4 °C. Following removal of mitochondria and nuclei, supernatants were layered onto 10–50% sucrose gradients and centrifuged at 38,000 rpm for 2 h at 4 °C in a SW40 rotor (Beckman Instruments). Gradients were fractionated into eleven 1 ml fractions using a density gradient fractionator system (Brandel Instruments). The profiles of the gradients were monitored at 260 nm, and RNAs from individual fractions pooled into a nonribosomal/monosomal pool and a polysomal pool. These RNAs (100 ng) were subsequently used in qRT-PCR analysis for the indicated transcripts using amplicons located within the coding region.

2.5. Immunoprecipitations, Immunoblot and *In Vitro* Methylation Assays

Immunoprecipitations and immunoblots were performed as described [18]. *In vitro* methylation reactions were performed by immunoprecipitating METTL3–14 complexes and used in 50 μl reactions containing 0.1 nM substrate RNA, 1 μCi of ^{3}H-labeled S-adenosyl-L-methionine, 80 mM KCl, 1.5 mM $MgCl_2$, 0.2 U/μl RNasin, 10 mM DTT, 4% glycerol and 15 mM HEPES (pH 7.9). Unincorporated ^{3}H S-adenosyl-L-methionine was removed using Qiaquick Spin columns (Qiagen) and incorporated radioactivity was measured by liquid scintillation counting.

2.6. hnRNP A1 *in vitro* Annealing Assays

Reactions were performed as described previously by Kumar and Wilson [22]. Briefly, a 19-mer oligonucleotide 5'-ACGGCCAGTGCCAAGCTTG-3' complementary to positions 6280 – 6298 on M13mp18(+) strand DNA was used as template in the annealing reactions. The oligonucleotide was 5'-end labeled and mixed with equimolar amounts (0.2 nM) of M13mp18 single-stranded DNA in the presence of native YTHDF3, hnRNP A1 or both proteins as indicated. Annealing reactions were allowed to proceed at 25 °C for 5 min and subsequently electrophoresed and the gels exposed to film.

2.7. Xenograft studies

All animal studies were performed in accordance with an approved Institutional Animal Care and Use Committee protocol. Male SCID mice were injected subcutaneously with single cell suspensions. Tumor growth was measured daily, and mice were randomized to PP242 versus vehicle when tumors reached 200 mm^3. Treatment was given by intraperitoneal injection for 5 days and tumor growth was assessed on day 8 or day 12 following initiation of PP242 treatment. IC_{50} was determined by extrapolation of plots of percent growth inhibition by PP242 versus log concentration.

2.8. Statistical analysis

Statistical analyses were performed using unpaired Student's *t* tests and one-way ANOVA using Systat 13 (Systat Software, Chicago, IL). *P* values of less then 0.05 were considered significant. Significance in group comparisons was determined using a one-way analysis of variance and data generated showed normal distribution with similar variances, and analysis was completed assuming equal variances.

3. Results

3.1. Relative differential sensitivity and dependence on the ITAF hnRNP A1 mediating resistance of GBM lines and short-term primary cultures to mTOR inhibition.

Our previous studies demonstrated that rapamycin and rapalogs significantly induced IRES-mediated translation of cyclin D1 and c-myc mRNAs following exposure [16, 20, 21]. The ability of these compounds to induce IRES activity of these two determinants was sufficient to render cells resistant to rapamycin in an AKT-dependent manner [21]. With the development of direct mTOR kinase inhibitors we were interested in whether generally these compounds would induce a similar response in GBM cells. We tested a panel of

established human GBM lines and patient-derived short term cultures for their relative sensitivity to the TORKI PP242 and identified 4 established GBM lines and 4 primary GBM cell cultures which displayed markedly differing sensitivities to the drug (Fig. 1A). Subsequently we determined whether resistance correlated with induced cyclin D1 and c-myc IRES activities. As shown in Fig. 1B, PP242 induced a robust cyclin D1 and c-myc IRES response that directly correlated with TORKI resistance while lines, which were relatively sensitive, displayed little or no IRES activity. Our previous work had also identified the ITAF hnRNP A1 as a regulatory factor whose cyclin D1 and c-myc IRES activating functions were inhibited by a serine 199 phosphorylation via AKT activity [17]. We also noted that irrespective of either harboring active or quiescent AKT, GBM lines treated with direct mTOR inhibitors displayed similar sensitivities, consistent with the ability of these compounds to block mTORC2-mediated AKT activation in most cell types. We subsequently determined whether the ITAF hnRNP A1 was required for TORKI-induced IRES activity and drug resistance. In resistant established ($U373MG_{(Uppsala)}$) or primary GBM (HK296) lines siRNA-mediated knockdown (Fig. 1C) or ectopic expression of a dominant negative shuttling-deficient hnRNP A1 mutant resulted in the inability to activate IRES-mediated translation initiation and conferred PP242 sensitivity to these lines (Figs. 1D–F).

3.2. Identification of m^{6}A-modifications in the cyclin D1 and c-myc IRESs which promote ITAF binding following mTOR inhibitor exposure.

N^6-methyladenosine is the most abundant internal modification which occurs cotranscriptionally in the context of a consensus RRACH/DRACH (D = G, A, or U; R = G or A; H = A, U, or C) sequence [23]. As recent data suggest that m^{6}A modification can regulate mRNA translation [24], we were interested if this modification may regulate IRES activity and mTOR inhibitor resistance. Interrogation of the datasets from two comprehensive analyses of the human and mouse m^{6}A mRNA methylomes [25] revealed three and two conserved DRACH motifs within the defined IRESs of the cyclin D1 and c-myc 5’ UTRs, respectively, which were sites of m^{6}A modification (Fig. 2A). These m^{6}A modification sites were also in close proximity to sequences containing consensus-binding motifs for the ITAF, hnRNP A1, which we have previously demonstrated to bind to the cyclin D1 and c-myc IRES RNAs [20] and were conserved within human and mouse sequences (Supplementary Fig. S1). We initially qualitatively tested whether oligonucleotides corresponding to these sequences, in which the adenosine was methylated, would display enhanced binding to hnRNP A1 *in vitro*. As shown in Fig. 2B, both the cyclin D1 and c-myc hairpin-loops displayed enhanced binding upon methylation of the adenosine indicated. To obtain quantitative binding data, we performed filter-binding studies which corroborated the RNA-pull down results. Each hairpin-loop bound increasing amounts (~ 7-fold average increase) of hnRNP A1 upon m^{6}A modification (Fig. 2C). These data identify DRACH m^{6}A-modification sites within the cyclin D1 and c-myc IRESs which upon methylation promote the association of the ITAF, hnRNP A1.

3.3. m^{6}A-modification stimulates IRES activity in mTOR inhibitor resistant cells.

To determine whether the endogenous cyclin D1 or c-myc IRESs displayed altered m^{6}A levels upon PP242 exposure we performed me-RIP analysis on treated cells and captured

RNAs quantified by qRT-PCR. As shown in Fig. 3A, PP242-resistant HK296 cells harbored elevated levels of m^6A cyclin D1 and c-myc IRES RNAs relative to untreated cells. In relatively sensitive T98G cells, no significant increases in m^6A-content was observed following treatment with PP242 in either cyclin D1 or c-myc transcripts. While other DRACH motifs are present within the cyclin D1 and c-myc transcripts, particularly within the 3' UTRs and near the stop codons, we did not detect additional sites of m^6A modification in response to mTOR inhibition in HK296 cells (not shown). We subsequently determined whether heterologous reporter mRNAs containing either the cyclin D1 or c-myc IRES sequences immediately upstream of the luciferase coding region would also display altered m^6A-content in PP242-resistant versus sensitive cells upon inhibitor exposure. As shown in Fig. 3B, these monocistronic luciferase reporter mRNAs displayed increased m^6A-content in PP242-resistant HK296 GBM cells, while in sensitive cells no significant increase was observed. While these observations suggest elevated m^6A modifications within the cyclin D1 and c-myc IRES RNAs, to determine specifically whether the adenosines in the hairpin-loops were necessary for IRES activity, we mutated each of the respective m^6A sites to U within the cyclin D1 and c-myc hairpin-loops and determined whether m^6A levels were altered in response to PP242 in resistant cells. Mutation of the m^6A sites, as indicated in Fig. 3C within the 3 c-myc IRES or 2 cyclin D1 hairpin-loops, resulted in marked reductions in IRES-based reporter mRNA m^6A-content. Mutation of each of the 3 c-myc hairpin adenosines individually rendered partial reductions in m^6A-content, however a mutant in which all three hairpin adenosines were mutated displayed dramatically lower levels of m^6A-content. Similar effects of m^6A site mutation were observed in the cyclin D1 hairpins. Individual mutation yielded only partial reductions, while mutating both adenosines markedly reduced m^6A-levels. To determine the effects of m^6A mutation within the cyclin D1 and c-myc hairpin loops had on IRES activity, we generated a series of dicistronic constructs in which the m^6A site mutants were introduced within the intragenic region. As shown in Fig. 3D, PP242-induced IRES activity was reduced in each of the single mutants however was markedly inhibited in IRESs containing all 3 of the c-myc or both of the cyclin D1 m^6A-mutants. These data demonstrate that c-myc and cyclin D1 IRES m^6A content is differentially induced in mTOR inhibitor resistant cells following exposure. Furthermore, mutational analysis of the cyclin D1 and c-myc IRES DRACH motifs support their methylation as a direct requirement for mTOR inhibitor induced IRES activity.

3.4. The METTL3–14/WTAP methyltransferase complex components increase in expression and methyltransferase activity is stimulated in resistant cells.

To begin to examine the mechanism by which elevated m^6A-modifications were observed within the IRESs in mTOR inhibitor resistant GBM cells following exposure, we determined whether the core m^6A methyltransferase complex was affected by PP242. As m^6A methylation is a dynamic reversible modification we also assessed whether the major m^6A demethylases FTO and ALKBH5 were affected by mTOR inhibitor exposure in these cells. As shown in Fig. 4A, in both $U373MG_{(Uppsala)}$ and HK296 cells, METTL3, METTL14 and WTAP components are induced following PP242 exposure at both the protein and mRNA levels. FTO and ALKBH5 expression was unaffected by PP242 treatment in either cell line. Induction of METTL3, METTL14 or WTAP expression was not observed in PP242 sensitive GBM cells and in fact, was markedly reduced (Supplementary Fig. S2). Moreover, METTL3

methyltransferase activity was coordinately stimulated in response to mTOR inhibition in resistant cells (Fig. 4B).

3.5. Silencing the m^{6}A-methylosome inhibits IRES activity and sensitizes mTOR inhibitor resistant cells.

We next investigated whether the m^{6}A methyltransferases METTL3–14 were required for induction of IRES activity in mTOR inhibitor resistant GBM cells. Silencing of the METTL3–14 enzymes via transfection of a pooled METTL3–14 targeting and a non-targeting scrambled sequence control siRNAs (Fig. 5A) resulted in significant inhibition of PP242-induced cyclin D1 or c-myc IRES activity in U373MG$_{(Uppsala)}$ (Fig. 5B, left panel) or in HK296 (Fig. 5B, right panel). Moreover, the mRNA translational states of the IRES-containing cyclin D1 and c-myc transcripts were determined in polysome analyses following METTL3–14 knockdown. As shown in Supplementary Figure S3, PP242 exposure in control non-targeting siRNA treated cells, induced a marked shift in cyclin D1 and c-myc mRNAs from relatively poorly translated nonribosomal/monosomal fractions to well translated polysomal fractions in these resistant lines. However, following knockdown of METTL3–14, this increase in the translational efficiencies of these transcripts was not observed in response to PP242 consistent with the inhibition of IRES activity. Depletion of METTL3–14 following 48 h post-transfection with METTL3–14 siRNAs additionally resulted in the sensitization of mTOR inhibitor resistant GBM lines to PP242 (Fig. 5C; see also Fig. 1A). These data demonstrate that RNAi-mediated knockdown of METTL3–14 proteins results in abrogation of mTOR inhibitor-induced IRES activity and acquired PP242 sensitivity of resistant GBM cells.

3.6. YTHDF3 is essential for mTOR inhibitor induced IRES activity.

The m^{6}A binding proteins (YTH domain family proteins) recognize m^{6}A-modified mRNAs and regulate their stability and translational efficiency [26, 27]. Of the YTH family of proteins, the YTHDC2 protein is the only member containing an RNA helicase domain and is known to affect translation by resolving structural constrains of translating mRNAs, thus positioning YTHDC2 as a candidate [28]. Contrary to our expectations, we tested all known members of the YTH-domain family for binding to each of the DRACH motifs identified within the c-myc or cyclin D1 IRESs. As shown in Fig. 6A each of the three DRACH motifs identified within the c-myc IRES bound to only YTHDF3 in a PP242-dependent manner in U373MG$_{(Uppsala)}$ or HK296 cells. Similarly, the two DRACH motifs identified in the cyclin D1 IRES sequences were found to associate specifically with YTHDF3 following PP242 treatment of U373MG$_{(Uppsala)}$ or HK296 GBM cells. We also examined whether YTHDF3 expression was induced by PP242 in GBM lines and as shown in Fig. 6C, YTHDF3 expression was markedly upregulated by PP242. As shown in Fig. 6D, siRNA-mediated knockdown of YTHDF3 resulted in marked sensitivity of mTOR inhibitor resistant GBM lines and significantly reduced IRES activity (Fig. 6E) as well as cyclin D1 and c-myc protein levels (Supplementary Figure S4) in U373MG$_{(Uppsala)}$ and HK296 cells. To determine whether knockdown of YTHDF3 also affected the sensitivity of U373$_{(Uppsala)}$ cells to PP242 in murine xenografts we generated cells stably expressing two distinct shRNAs targeting YTHDF3 (shYTHDF3–1, shYTHDF3–2). PP242-induced YTHDF3 expression was markedly reduced in these cells (Supplementary Fig. 5A). Mice

were injected with U373MG$_{(Uppsala)}$ expressing either vector, a non-targeting scrambled sequence shRNA, or cells expressing one of two YTHDF3-targeting shRNAs. Upon tumors reaching a mean volume of 200 mm^3, all the mice were given PP242 (vehicle, 0.1, 4 and 10 mg/kg/d) each day for five consecutive days, and at 8 and 12 days following initiation of treatment tumor growth was assessed. As shown in Supplementary Fig. 5B, PP242 inhibited the growth of all cell lines in a dose dependent fashion. However, xenografted U373MG$_{(Uppsala)}$ tumors expressing either shYTHDF3-targeting shRNAs were significantly more sensitive to PP242 as compared to tumors transduced with vector only or control scrambled non-targeting shRNA. We also determined m^{6}A cyclin D1 and c-myc IRES RNA and protein levels in harvested tumors. While the relative m^{6}A levels increased in a dose-dependent manner following PP242 treatment in all the tumors (Supplementary Figure S5C), protein levels of cyclin D1 and c-myc increased in control and nontargeting shRNA expressing tumors and decreased or were undetectable in tumors expressing either of the two YTHDF3-targeting shRNAs (Supplementary Figure S5D). These data demonstrate that YTHDF3 specifically associates with the DRACH motifs from the c-myc and cyclin D1 IRESs and its expression is induced following mTOR inhibitor treatment. Moreover, YTHDF3 is required for IRES activity and depletion of this YTH family member sensitizes mTOR inhibitor resistant cells *in vitro* and in xenograft experiments.

3.7. YTHDF3 interacts with hnRNP A1 and stimulates hnRNP A1-induced RNA strand induced annealing activity.

The requirement for YTHDF3 for mTOR inhibitor-induced IRES activity and previous data demonstrating that the ITAF hnRNP A1 can associate with m^{6}A modified RNA [29], suggested to us that these two RNA-binding proteins may cooperatively regulate IRES activity. To address this possibility we determined whether hnRNP A1 and YTHDF3 were interacting proteins, as several examples of cooperative regulation involve distinct interacting RNA-binding proteins [30]. As shown in Fig. 7A, in coimmunoprecipitation experiments of endogenous YTHDF3 and hnRNP A1, YTHDF3 efficiently coimmunoprecipitated hnRNP A1 (left panel) and in the reciprocal coimmunoprecipitation hnRNP A1 bound YTHDF3 (right panel). Our previous studies supported a role for hnRNP A1 in promoting strong annealing activity [17] and a critical function of this property may be to provide required structural elements which favor the formation of a competent IRES conformation capable of ribosome recruitment. As shown in Fig. 7B, recombinant YTHDF3 alone did not display annealing activity, while native hnRNP A1 promoted reannealing of a single-stranded M13 mp18 plus strand DNA and a complementary 19-mer oligonucleotide in an *in vitro* annealing assay. The addition of YTHDF3 to the annealing reaction markedly stimulated hnRNP A1-mediated reannealing and formation of annealed product. These data demonstrate that endogenous YTHDF3 and hnRNP A1 are interacting proteins and that YTHDF3 stimulates the annealing properties of the ITAF hnRNP A1.

4. Discussion

Several oncogenic signaling cascades are known to be altered in GBM contributing to the overall pathogenesis of the disease. mTOR has emerged as a promising therapeutic

target, however pharmacological inhibitors thusfar have yielded disappointing results in clinical trials. GBM heterogeneity, imperfect pharmacology of current inhibitors, and intrinsic, as well as, acquired drug resistance mechanisms have contributed to the poor performance of these drugs to date. Our previous studies have implicated a protein synthesis salvage pathway which is activated upon mTOR inhibition that directs the specific mRNA translation of critical transcripts resulting in drug resistance [16]. Our earlier studies demonstrated that the requisite ITAF, hnRNP A1 was preferentially symmetrically di-methylated on arginines 218 and 225 in the face of mTOR inhibition via induction of PRMT5 activity [19]. Here we have identified specific m^{6}A methylation sites within the cyclin D1 and c-myc IRES RNAs which are required to be modified in order to stimulate hnRNP A1-mediated IRES activity leading to drug resistance. Our analysis demonstrates that the m^{6}A-methylosome components METTL3–14 and WTAP are induced following PP242 exposure resulting in methylation of the cyclin D1 and c-myc IRESs. This post-transcriptional modification results in enhanced binding of the ITAF hnRNP A1 leading to elevated IRES activity and protein synthesis.

The m^{6}A modification is the most abundant internal post-transcriptional modification to mRNA [24]. Through the actions of methyltransferases, demethylases and methyl-binding proteins, these modifications are dynamic and reversible and can affect mRNA metabolic processes such as splicing, localization, stability and translation [29]. While m^{6}A modifications have been shown to promote IRES-mediated translation initiation in circular RNAs [31], to our knowledge, our study is the first to demonstrate stimulation of IRES activity in cellular mRNAs. m^{6}A modifications have been demonstrated to stimulate eIF3 mediated translation initiation in mRNAs, however this was shown to occur under default conditions of normal eIF-4F dependent translation initiation [32]. Our data also support the ability of specific m^{6}A-modifications to direct IRES-mediated translation under conditions of impaired cap-dependent translation initiation following mTOR inhibition.

We found that following treatment of GBM cell lines and PDX cultures with PP242, expression of the m^{6}A-methylation machinery was significantly increased with a concomitant stimulation of m^{6}A methylation activity. This is in contrast to a recent report of mTORC1 activating m^{6}A RNA methylation via effects on WTAP expression [33]. One potential explanation for this difference may involve the utilization of lines in our study that are resistant to mTOR inhibition and possibly harboring additional genetic alterations which may uncouple m^{6}A-methylosome component expression from mTORC1 activity. In fact, PP242 sensitive GBM lines (T98G and LN229) exhibited a reduction in m^{6}A-methylosome component expression following inhibitor exposure (see Supplementary Fig. 2). Moreover, we did not observe an increase in m^{6}A content of either the cyclin D1 or c-myc IRES reporters introduced into T98G cells following PP242 treatment (Fig. 3B). Future efforts will focus on elucidating the mechanism mediating this differential response.

We identified the YTH-domain containing protein YTHDF3 as preferentially associating with m^{6}A-modified cyclin D1 and c-myc IRES RNA following mTOR inhibitor exposure. The fate and function of m^{6}A-modified transcripts are mediated through “reader” proteins including the YTH family proteins affecting mRNA translation among other properties. Numerous studies have reported that YTHDF3 promotes the translational efficiency of its

target mRNAs and is dependent on m^{6}A recognition [34, 35]. Autoregulation of YTHDF3 via cap-independent translation requiring m^{6}A modifications within its own 5' UTR has also been described [36]. Our data clearly support a role for YTHDF3 in stimulating IRES-dependent translation. Additionally, we observed a direct interaction of endogenous YTHDF3 with the ITAF hnRNP A1 which in combination, stimulated the *in vitro* nucleic acid annealing activity of hnRNP A1. This property has been proposed to facilitate the formation of a competent IRES structure capable of 40S ribosomal subunit recruitment [17, 37, 38]. Cooperative RNA-binding protein interactions which affect translational control have been previously observed. A complex consisting of hnRNP A0, hnRNP A2, and ELAV1 associates with the 5' UTR of the ANXA2R transcript to regulate its translational efficiency [39]. Similarly, the DEAD-box helicase DDX3X and Calprin-1 form a complex and associate with structured mRNA leaders to control translation through PABP1 promoting cell spreading and motility in fibroblasts [40]. m^{6}A-modifications have been demonstrated to behave as RNA structural switches regulating how RBPs gain access to their specific binding motifs [41]. It is likely that the m^{6}A methylations observed within the IRESs of the cyclin D1 and c-myc following mTOR inhibitor exposure regulate YTHDF3/hnRNP A1 complex binding and subsequent ITAF activity.

Taken together with our previous findings, our data suggest that mTOR inhibitor-induced IRES activity is a dynamic and complex process involving both IRES RNA and ITAF modifications to stimulate IRES-dependent protein synthesis resulting in mTOR inhibitor resistance. Impinging on this process we have identified m^{6}A-modification of IRES-containing RNAs, as well as, both arginine methylation and site-specific phosphorylation of hnRNP A1 as contributory to this regulation [19, 20]. Akin to the regulation of transcription by DNA methylation and histone methylation/acetylation modifications, in which crosstalk mechanisms have been found to govern gene expression at this level, it is possible that IRES-mediated translation initiation is subject to similar controls and crosstalk regulatory mechanisms [42]. Understanding these relationships will be necessary in order to design effective cotherapies to overcome mTOR inhibitor resistance.

Supplementary Material

Refer to Web version on PubMed Central for supplementary material.

Acknowledgements

We thank Drs Norimoto Yanagawa, Harley Kornblum, Paul Mischel and Danilo Perrotti for reagents. We also thank Dr Alan Lichtenstein for comments on the manuscript. This work was supported, in whole or in part, by VA MERIT I01BX002665 and NIH R01CA217820 grants.

Author's Disclosures

J. Gera reports other support from the Jean Ferguson Endowment at UCLA. No disclosures were reported by the other authors.

List of Abbreviations:

GBM	glioblastoma

IRES	internal ribosome entry site
ITAF	IRES-*trans*-acting factor
TORKI	TOR kinase inhibitor
hnRNP A1	heterogeneous nuclear ribonucleoprotein A1
m^{6}A	N^6-methyladenosine
mTOR	mechanistic target of rapamycin kinase
METTL3	N^6-adenosine-methyltransferase catalytic subunit
METTL14	N^6-adenosine-methyltransferase non-catalytic subunit
WTAP	Wilms' tumor 1-associating protein
FTO	Fat mass and obesity-associated protein
ALKBH5	AlkB homolog H5
YTHDF3	YTH N^6-Methyladenosine RNA Binding Protein 3

References

[1]. Cloughesy TF, Cavenee WK, Mischel PS, Glioblastoma: from molecular pathology to targeted treatment, Annual review of pathology, 9 (2014) 1–25.

[2]. Omuro A, DeAngelis LM, Glioblastoma and other malignant gliomas: a clinical review, Jama, 310 (2013) 1842–1850. [PubMed: 24193082]

[3]. Oronsky B, Reid TR, Oronsky A, Sandhu N, Knox SJ, A Review of Newly Diagnosed Glioblastoma, Frontiers in oncology, 10 (2020) 574012. [PubMed: 33614476]

[4]. Dymova MA, Kuligina EV, Richter VA, Molecular Mechanisms of Drug Resistance in Glioblastoma, International journal of molecular sciences, 22 (2021).

[5]. Brennan CW, Verhaak RG, McKenna A, Campos B, Noushmehr H, Salama SR, Zheng S, Chakravarty D, Sanborn JZ, Berman SH, Beroukhim R, Bernard B, Wu CJ, Genovese G, Shmulevich I, Barnholtz-Sloan J, Zou L, Vegesna R, Shukla SA, Ciriello G, Yung WK, Zhang W, Sougnez C, Mikkelsen T, Aldape K, Bigner DD, Van Meir EG, Prados M, Sloan A, Black KL, Eschbacher J, Finocchiaro G, Friedman W, Andrews DW, Guha A, Iacocca M, O'Neill BP, Foltz G, Myers J, Weisenberger DJ, Penny R, Kucherlapati R, Perou CM, Hayes DN, Gibbs R, Marra M, Mills GB, Lander E, Spellman P, Wilson R, Sander C, Weinstein J, Meyerson M, Gabriel S, Laird PW, Haussler D, Getz G, Chin L, The somatic genomic landscape of glioblastoma, Cell, 155 (2013) 462–477. [PubMed: 24120142]

[6]. Fan QW, Weiss WA, Targeting the RTK-PI3K-mTOR axis in malignant glioma: overcoming resistance, Current topics in microbiology and immunology, 347 (2010) 279–296. [PubMed: 20535652]

[7]. Akhavan D, Cloughesy TF, Mischel PS, mTOR signaling in glioblastoma: lessons learned from bench to bedside, Neuro-oncology, 12 (2010) 882–889. [PubMed: 20472883]

[8]. González A, Hall MN, Nutrient sensing and TOR signaling in yeast and mammals, The EMBO journal, 36 (2017) 397–408. [PubMed: 28096180]

[9]. Liu GY, Sabatini DM, mTOR at the nexus of nutrition, growth, ageing and disease, Nature reviews. Molecular cell biology, 21 (2020) 183–203. [PubMed: 31937935]

[10]. Fan QW, Nicolaides TP, Weiss WA, Inhibiting 4EBP1 in Glioblastoma, Clinical cancer research : an official journal of the American Association for Cancer Research, 24 (2018) 14–21.

[11]. Thoreen CC, Sabatini DM, Rapamycin inhibits mTORC1, but not completely, Autophagy, 5 (2009) 725–726. [PubMed: 19395872]

[12]. Chen X, Liu M, Tian Y, Li J, Qi Y, Zhao D, Wu Z, Huang M, Wong CCL, Wang HW, Wang J, Yang H, Xu Y, Cryo-EM structure of human mTOR complex 2, Cell research, 28 (2018) 518–528. [PubMed: 29567957]

[13]. Shi Y, Yan H, Frost P, Gera J, Lichtenstein A, Mammalian target of rapamycin inhibitors activate the AKT kinase in multiple myeloma cells by up-regulating the insulin-like growth factor receptor/insulin receptor substrate-1/phosphatidylinositol 3-kinase cascade, Molecular cancer therapeutics, 4 (2005) 1533–1540. [PubMed: 16227402]

[14]. O'Reilly KE, Rojo F, She QB, Solit D, Mills GB, Smith D, Lane H, Hofmann F, Hicklin DJ, Ludwig DL, Baselga J, Rosen N, mTOR inhibition induces upstream receptor tyrosine kinase signaling and activates Akt, Cancer research, 66 (2006) 1500–1508. [PubMed: 16452206]

[15]. Rodrik-Outmezguine VS, Okaniwa M, Yao Z, Novotny CJ, McWhirter C, Banaji A, Won H, Wong W, Berger M, de Stanchina E, Barratt DG, Cosulich S, Klinowska T, Rosen N, Shokat KM, Overcoming mTOR resistance mutations with a new-generation mTOR inhibitor, Nature, 534 (2016) 272–276. [PubMed: 27279227]

[16]. Holmes B, Lee J, Landon KA, Benavides-Serrato A, Bashir T, Jung ME, Lichtenstein A, Gera J, Mechanistic Target of Rapamycin (mTOR) Inhibition Synergizes with Reduced Internal Ribosome Entry Site (IRES)-mediated Translation of Cyclin D1 and c-MYC mRNAs to Treat Glioblastoma, The Journal of biological chemistry, 291 (2016) 14146–14159. [PubMed: 27226604]

[17]. Martin J, Masri J, Cloninger C, Holmes B, Artinian N, Funk A, Ruegg T, Anderson L, Bashir T, Bernath A, Lichtenstein A, Gera J, Phosphomimetic substitution of heterogeneous nuclear ribonucleoprotein A1 at serine 199 abolishes AKT-dependent internal ribosome entry site-transacting factor (ITAF) function via effects on strand annealing and results in mammalian target of rapamycin complex 1 (mTORC1) inhibitor sensitivity, The Journal of biological chemistry, 286 (2011) 16402–16413. [PubMed: 21454539]

[18]. Benavides-Serrato A, Saunders JT, Holmes B, Nishimura RN, Lichtenstein A, Gera J, Repurposing Potential of Riluzole as an ITAF Inhibitor in mTOR Therapy Resistant Glioblastoma, International journal of molecular sciences, 21 (2020).

[19]. Holmes B, Benavides-Serrato A, Saunders JT, Landon KA, Schreck AJ, Nishimura RN, Gera J, The protein arginine methyltransferase PRMT5 confers therapeutic resistance to mTOR inhibition in glioblastoma, Journal of neuro-oncology, 145 (2019) 11–22. [PubMed: 31473880]

[20]. Jo OD, Martin J, Bernath A, Masri J, Lichtenstein A, Gera J, Heterogeneous nuclear ribonucleoprotein A1 regulates cyclin D1 and c-myc internal ribosome entry site function through Akt signaling, The Journal of biological chemistry, 283 (2008) 23274–23287. [PubMed: 18562319]

[21]. Shi Y, Sharma A, Wu H, Lichtenstein A, Gera J, Cyclin D1 and c-myc internal ribosome entry site (IRES)-dependent translation is regulated by AKT activity and enhanced by rapamycin through a p38 MAPK- and ERK-dependent pathway, The Journal of biological chemistry, 280 (2005) 10964–10973. [PubMed: 15634685]

[22]. Kumar A, Wilson SH, Studies of the strand-annealing activity of mammalian hnRNP complex protein A1, Biochemistry, 29 (1990) 10717–10722. [PubMed: 1703006]

[23]. Huang H, Weng H, Chen J, The Biogenesis and Precise Control of RNA m(6)A Methylation, Trends in genetics : TIG, 36 (2020) 44–52. [PubMed: 31810533]

[24]. Meyer KD, m(6)A-mediated translation regulation, Biochimica et biophysica acta. Gene regulatory mechanisms, 1862 (2019) 301–309. [PubMed: 30342175]

[25]. Liu J, Li K, Cai J, Zhang M, Zhang X, Xiong X, Meng H, Xu X, Huang Z, Peng J, Fan J, Yi C, Landscape and Regulation of m(6)A and m(6)Am Methylome across Human and Mouse Tissues, Molecular cell, 77 (2020) 426–440.e426. [PubMed: 31676230]

[26]. Wang X, Zhao BS, Roundtree IA, Lu Z, Han D, Ma H, Weng X, Chen K, Shi H, He C, N(6)-methyladenosine Modulates Messenger RNA Translation Efficiency, Cell, 161 (2015) 1388–1399. [PubMed: 26046440]

[27]. Liao S, Sun H, Xu C, YTH Domain: A Family of N(6)-methyladenosine (m(6)A) Readers, Genomics, proteomics & bioinformatics, 16 (2018) 99–107.

[28]. Xu Y, Zhang W, Shen F, Yang X, Liu H, Dai S, Sun X, Huang J, Guo Q, YTH Domain Proteins: A Family of m(6)A Readers in Cancer Progression, Frontiers in oncology, 11 (2021) 629560. [PubMed: 33692959]

[29]. Dominissini D, Moshitch-Moshkovitz S, Schwartz S, Salmon-Divon M, Ungar L, Osenberg S, Cesarkas K, Jacob-Hirsch J, Amariglio N, Kupiec M, Sorek R, Rechavi G, Topology of the human and mouse m6A RNA methylomes revealed by m6A-seq, Nature, 485 (2012) 201–206. [PubMed: 22575960]

[30]. Dassi E, Handshakes and Fights: The Regulatory Interplay of RNA-Binding Proteins, Frontiers in molecular biosciences, 4 (2017) 67. [PubMed: 29034245]

[31]. Yang Y, Fan X, Mao M, Song X, Wu P, Zhang Y, Jin Y, Yang Y, Chen LL, Wang Y, Wong CC, Xiao X, Wang Z, Extensive translation of circular RNAs driven by N(6)-methyladenosine, Cell research, 27 (2017) 626–641. [PubMed: 28281539]

[32]. Meyer KD, Patil DP, Zhou J, Zinoviev A, Skabkin MA, Elemento O, Pestova TV, Qian SB, Jaffrey SR, 5' UTR m(6)A Promotes Cap-Independent Translation, Cell, 163 (2015) 999–1010. [PubMed: 26593424]

[33]. Cho S, Lee G, Pickering BF, Jang C, Park JH, He L, Mathur L, Kim SS, Jung S, Tang HW, Monette S, Rabinowitz JD, Perrimon N, Jaffrey SR, Blenis J, mTORC1 promotes cell growth via m(6)A-dependent mRNA degradation, Molecular cell, 81 (2021) 2064–2075.e2068. [PubMed: 33756105]

[34]. Coots RA, Liu XM, Mao Y, Dong L, Zhou J, Wan J, Zhang X, Qian SB, m(6)A Facilitates eIF4F-Independent mRNA Translation, Molecular cell, 68 (2017) 504–514.e507. [PubMed: 29107534]

[35]. Shi H, Wang X, Lu Z, Zhao BS, Ma H, Hsu PJ, Liu C, He C, YTHDF3 facilitates translation and decay of N(6)-methyladenosine-modified RNA, Cell research, 27 (2017) 315–328. [PubMed: 28106072]

[36]. Chang G, Shi L, Ye Y, Shi H, Zeng L, Tiwary S, Huse JT, Huo L, Ma L, Ma Y, Zhang S, Zhu J, Xie V, Li P, Han L, He C, Huang S, YTHDF3 Induces the Translation of m(6)A-Enriched Gene Transcripts to Promote Breast Cancer Brain Metastasis, Cancer cell, 38 (2020) 857–871.e857. [PubMed: 33125861]

[37]. Mitchell SA, Spriggs KA, Coldwell MJ, Jackson RJ, Willis AE, The Apaf-1 internal ribosome entry segment attains the correct structural conformation for function via interactions with PTB and unr, Molecular cell, 11 (2003) 757–771. [PubMed: 12667457]

[38]. Pickering BM, Mitchell SA, Spriggs KA, Stoneley M, Willis AE, Bag-1 internal ribosome entry segment activity is promoted by structural changes mediated by poly(rC) binding protein 1 and recruitment of polypyrimidine tract binding protein 1, Molecular and cellular biology, 24 (2004) 5595–5605. [PubMed: 15169918]

[39]. Zhang J, Kong L, Guo S, Bu M, Guo Q, Xiong Y, Zhu N, Qiu C, Yan X, Chen Q, Zhang H, Zhuang J, Wang Q, Zhang SS, Shen Y, Chen M, hnRNPs and ELAVL1 cooperate with uORFs to inhibit protein translation, Nucleic acids research, 45 (2017) 2849–2864. [PubMed: 27789685]

[40]. Copsey AC, Cooper S, Parker R, Lineham E, Lapworth C, Jallad D, Sweet S, Morley SJ, The helicase, DDX3X, interacts with poly(A)-binding protein 1 (PABP1) and caprin-1 at the leading edge of migrating fibroblasts and is required for efficient cell spreading, The Biochemical journal, 474 (2017) 3109–3120. [PubMed: 28733330]

[41]. Liu N, Dai Q, Zheng G, He C, Parisien M, Pan T, N(6)-methyladenosine-dependent RNA structural switches regulate RNA-protein interactions, Nature, 518 (2015) 560–564. [PubMed: 25719671]

[42]. Murr R, Interplay between different epigenetic modifications and mechanisms, Advances in genetics, 70 (2010) 101–141. [PubMed: 20920747]

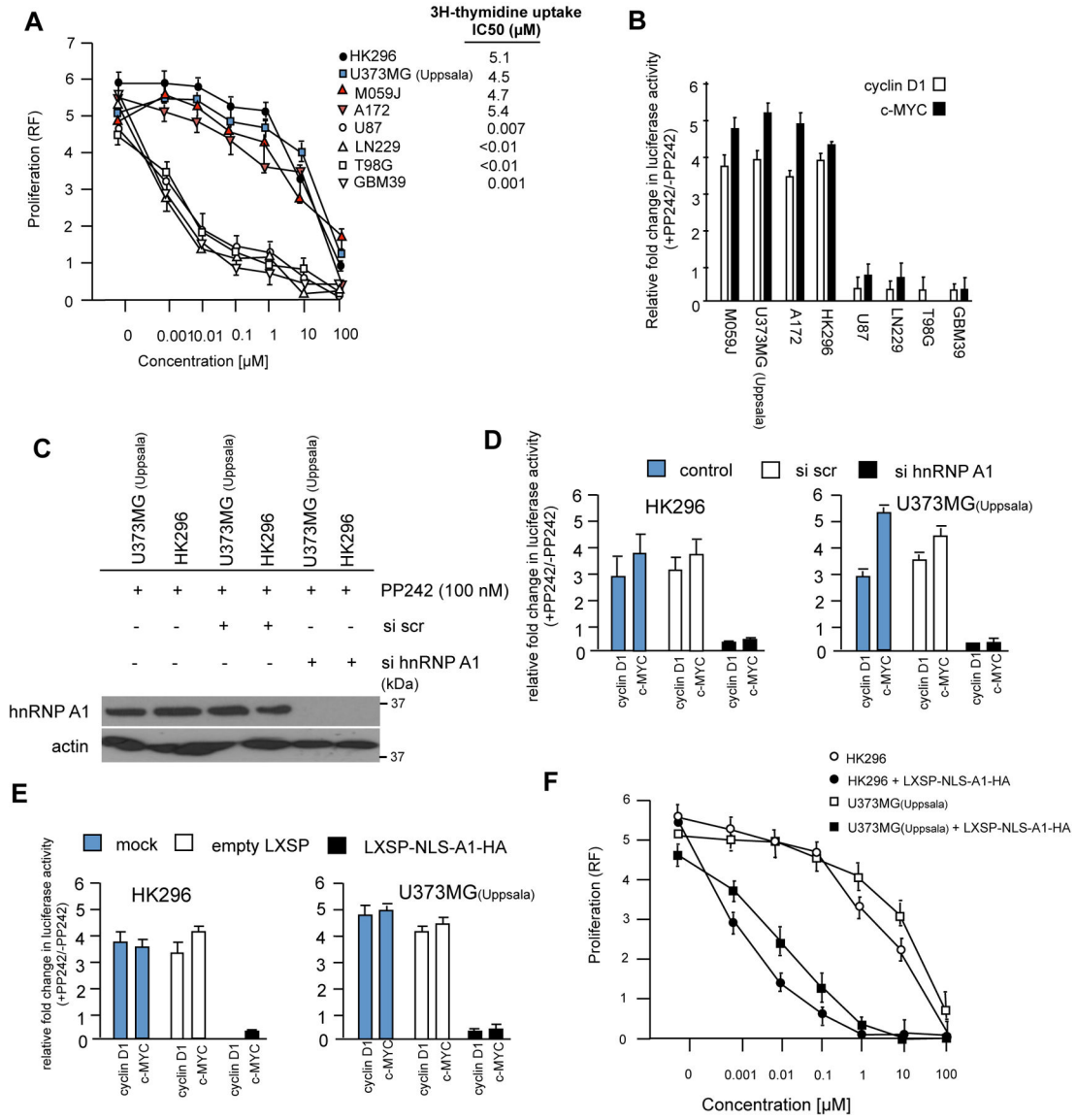

Fig. 1.

Differential sensitivity and dependence on the ITAF hnRNP A1 mediating resistance of GBM lines and short-term primary cultures to PP242. **(A)** Dose-response curves of the indicated lines following 48 h exposure to PP242. IC_{50} for resistant cells ranged from 10 – 4.5 μM, while those for sensitive cells ranged from 7 – 12 nM. Proliferation was measured using resazurin. IC_{50}'s as determined via ^{3}H-thymidine uptake assays for each cell line treated with a range of PP242 concentrations are shown to the right of the graph. Mean ± S.D. are shown, n = 3. **(B)** Relative cyclin D1 and c-myc IRES activities of the indicated GBM lines following 48 h exposure to PP242. Relative fold change in IRES activity derived from dicistronic IRES mRNA reporter assays [20], in which plasmids containing the respective IRES sequences drive IRES dependent translation of Firefly luciferase is shown compared with luciferase activities obtained in the absence of PP242. **(C)** The ITAF hnRNP A1 is required for PP242-induced IRES activity and drug resistance.

siRNA-mediated knockdown of hnRNP A1 in U373MG$_{(Uppsala)}$ and primary HK296 cells. Cells were transiently transfected with siRNAs targeting hnRNP A1 or a nontargeting scrambled (scr) sequence and exposed to PP242 for 24 h and immunoblotted for the indicated proteins. **(D)** Effects of hnRNP A1 knockdown on PP242-induced IRES activity. U373MG$_{(Uppsala)}$ (*right panel*) or HK296 (*left panel*) were transiently transfected with the indicated siRNAs and IRES mRNA reporters and treated with PP242 as shown. Relative fold change in Firefly luciferase activity is shown in the presence of PP242 compared with values obtained in its absence. Mean + S.D. are shown, n = 3. **(E)** Effects of a dominant-negative shuttling-deficient hnRNP A1 mutant on PP242-induced IRES activity in stably transduced HK296 (*left panel*) and U373MG$_{(Uppsala)}$ (*right panel*) cells. The mean and + S.D. are shown for three independent experiments. **(F)** Ectopic expression of the dominant-negative hnRNP A1 shuttling-deficient mutant confers sensitivity to PP242. The indicated cells stably transduced with the hnRNP A1 mutant was treated with a range of concentrations for 48 h and subsequently proliferation was determined using resazurin. Mean ± S.D. are shown, n = 3.

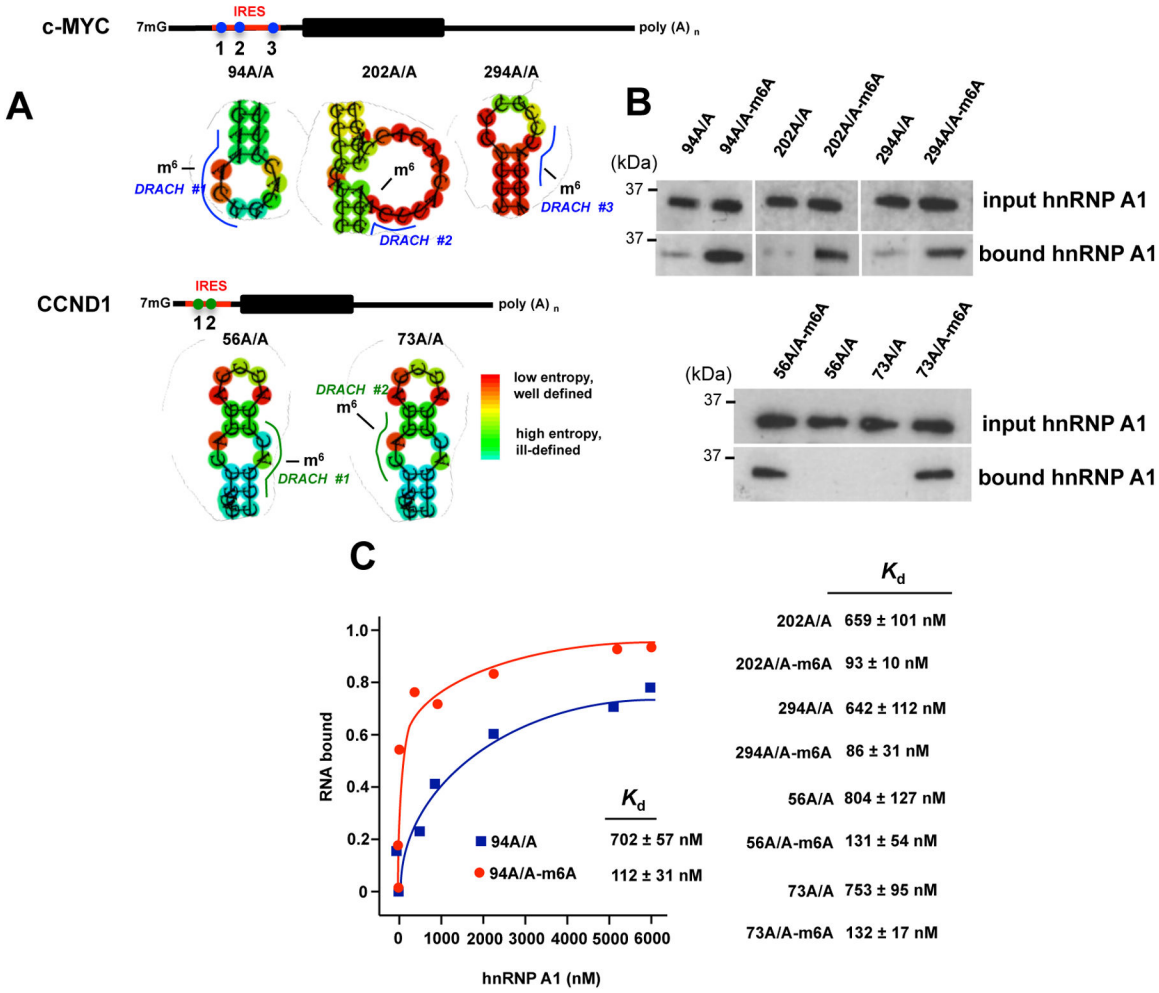

Fig. 2.

Site-specific m^{6}A modification of the cyclin D1 and c-myc IRESs increases hnRNP A1 binding. **(A)** Schematic of mRNAs, sequences and predicted hairpin structures within the cyclin D1 and c-myc IRESs as indicated. The c-myc IRES harbors three, while the cyclin D1 harbors two well conserved structural motifs containing DRACH (c-myc, blue; cyclin D1 green) sequences as shown. **(B)** RNA-pull down assays demonstrating that hnRNP A1 preferentially binds m^{6}A methylated cyclin D1 or c-myc IRES RNAs. Biotin conjugated oligonucleotides containing a m^{6}A modification at the appropriate adenosine within the indicated DRACH motifs were used in binding reactions of U373MG$_{(Uppsala)}$ cell lysates and immunoprecipitated using streptavidin coated beads. Immunoprecipitates and input lysates were immunoblotted for hnRNP A1 as indicated. **(C)** Filter-binding assays showing that m^{6}A modification increases hnRNP A1 binding of the indicated hairpin-loop DRACH containing motifs from the cyclin D1 or c-myc IRESs. The respective dissociation constants (*K*d) are indicated in the right panel. Data are mean ± S.D.; n = 3.

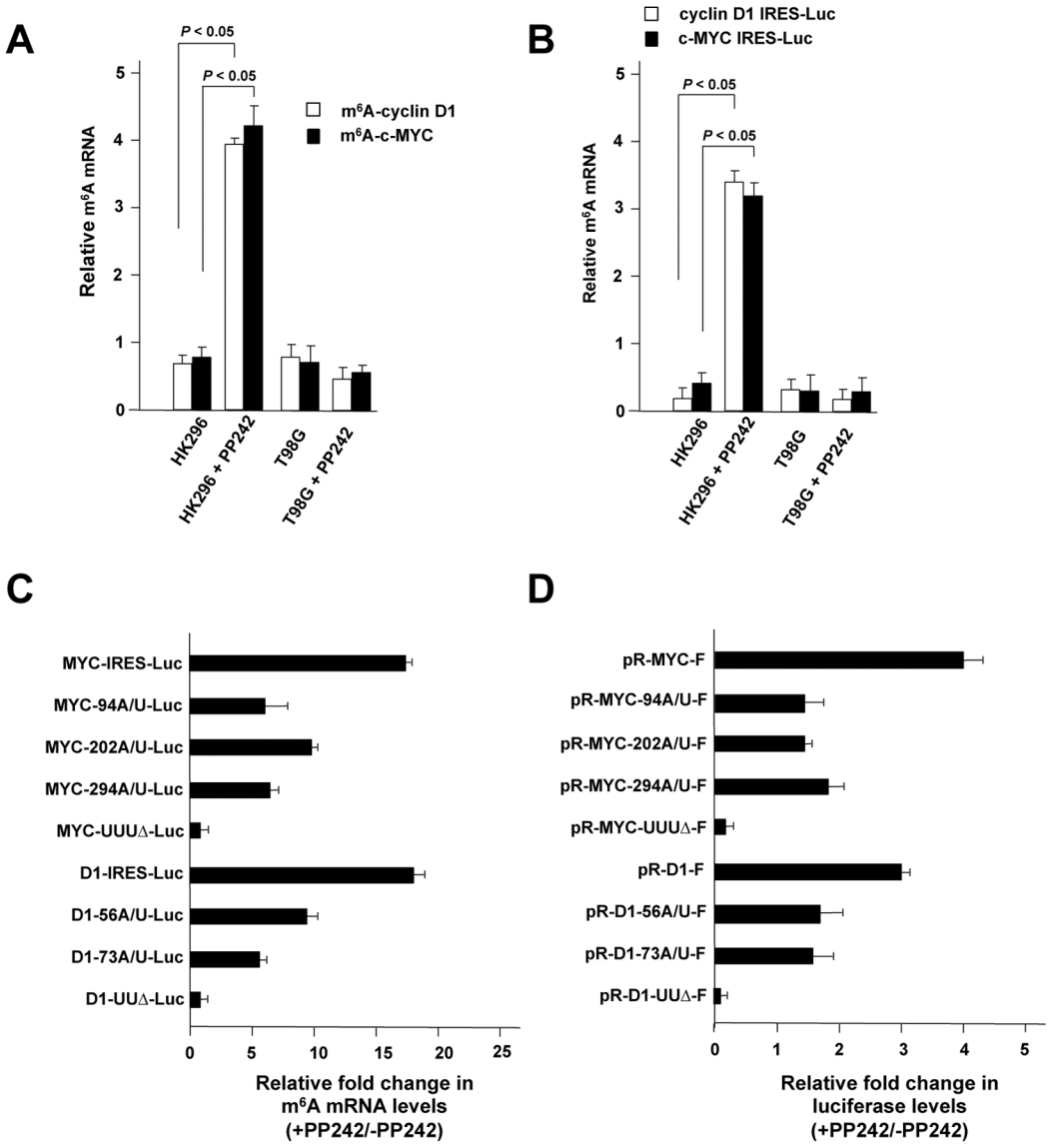

Fig. 3.

Cyclin D1 and c-myc IRES m^6A content is elevated in mTOR inhibitor resistant GBM cells following exposure. **(A)** Cyclin D1 and c-myc IRES m^6A content in HK296 (PP242 resistant) and T98G (PP242 sensitive) cells following exposure to PP242 (100 nM, 4 h). RNAs were extracted from treated cells and immunoprecipitated using α-m^6A antibodies. m^6A-RNA levels were subsequently determined via qRT-PCR. PCR reactions were performed in quadruplicate and mean + S.D. is shown. *P*-values are indicated. **(B)** As in **(A)** except the indicated cell lines were transfected with either a monocistronic cyclin D1-IRES-luciferase or c-myc-IRES-luciferase mRNA reporter. **(C)** Relative fold change in m^6A-content of the indicated native and mutant IRES RNAs in $U373MG_{(Uppsala)}$ cells in the presence versus absence of PP242 (100 nM, 4h). Mean + S.D. are shown; n = 3. **(D)** Relative IRES activities of the native cyclin D1 and c-myc IRESs as compared to the indicated hairpin-loop mutants. Relative fold change in IRES activity is shown in the presence versus

absence of PP242 treatment in U373MG$_{(Uppsala)}$ cells (100 nM, 4 h). Mean + S.D. are shown; n = 3.

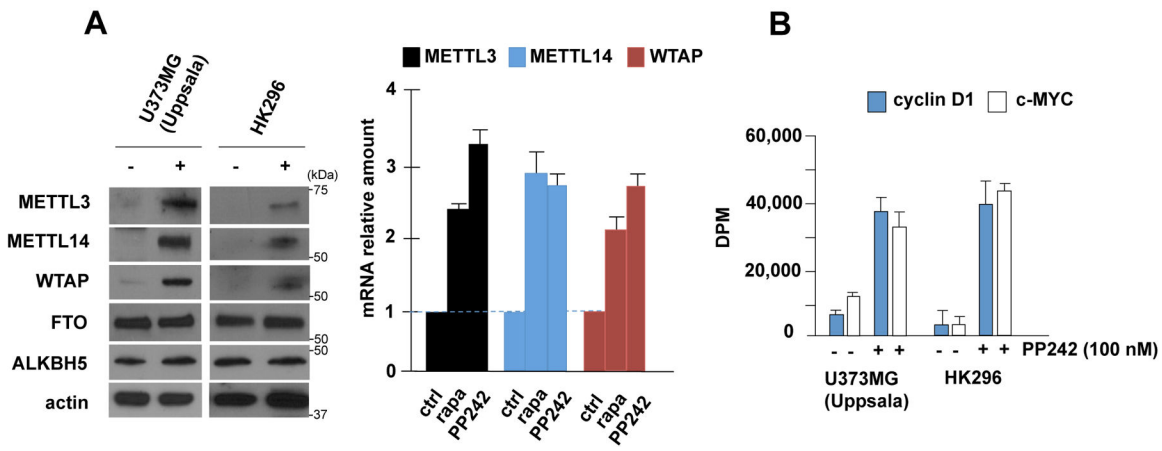

Fig. 4.

METTL3–14/WTAP methyltransferase complex expression and activity following mTOR inhibitor exposure in GBM. **(A)** METTL3, METTL14, WTAP, FTO, ALKBH5 and actin expression following PP242 exposure (100 nM, 18 h) in U373MG$_{(Uppsala)}$ and HK296 cells, *left panel*. Relative mRNA levels of METTL3, METTL14 and WTAP as determined by qrt-PCR following treatment of U373MG$_{(Uppsala)}$ cells with rapamycin (rapa) (100 nM, 18 h) or PP242 (100 nM, 18 h) as indicated, Mean + S.D., n = 4, *right panel*. **(B)** *In vitro* METTL3–14 activity of the indicated cells following exposure to PP242 as indicated (18 h). c-myc 294 A/A or cyclin D1 73 A/A RNAs were used as substrates in *in vitro* methylation reactions containing ^{3}H-labeled SAM-e. Mean + S.D., n = 3.

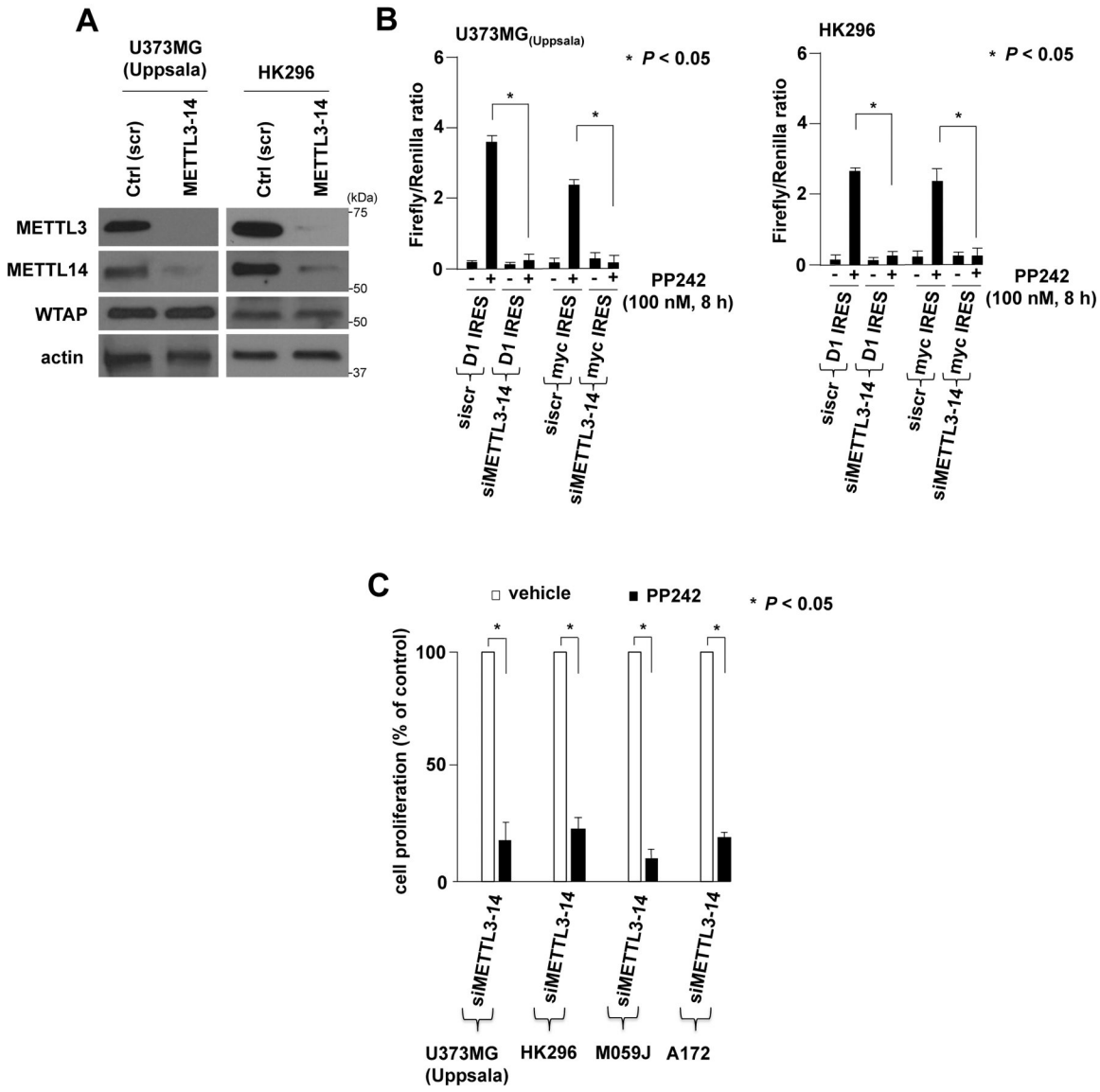

Fig. 5.

Silencing the m^{6}A-methylosome blocks IRES activity and leads to mTOR inhibitor sensitivity of resistant GBM tumor cells. **(A)** RNAi-mediated knockdown of METTL3–14 following transfection of U373MG$_{(Uppsala)}$ or HK296 cells with pooled siRNAs targeting both METTL3 and METTL14 or a non-targeting scrambled control sequence as shown. Lysates were immunoblotted for the indicated proteins. **(B)** Cyclin D1 or c-myc IRES activity in U373MG$_{(Uppsala)}$ (*left panel)* or HK296 (*right panel*) following knockdown of METTL3–14 and treatment with PP242. Activity is displayed as relative Firefly/Renilla luciferase activity from a dicistronic mRNA reporter. Luciferase activity was normalized to the luciferase mRNA level. * *P*-values are shown. Mean + S.D.; n = 3. **(C)** Knockdown of METTL3–14 sensitizes PP242-resistant GBM cells. ATP-release assays (Promega CellTiter-Glo® assay) were used to quantify proliferation and displayed as percent of vehicle alone control treatments. * *P*-values are shown. Mean + S.D. are shown; n = 3.

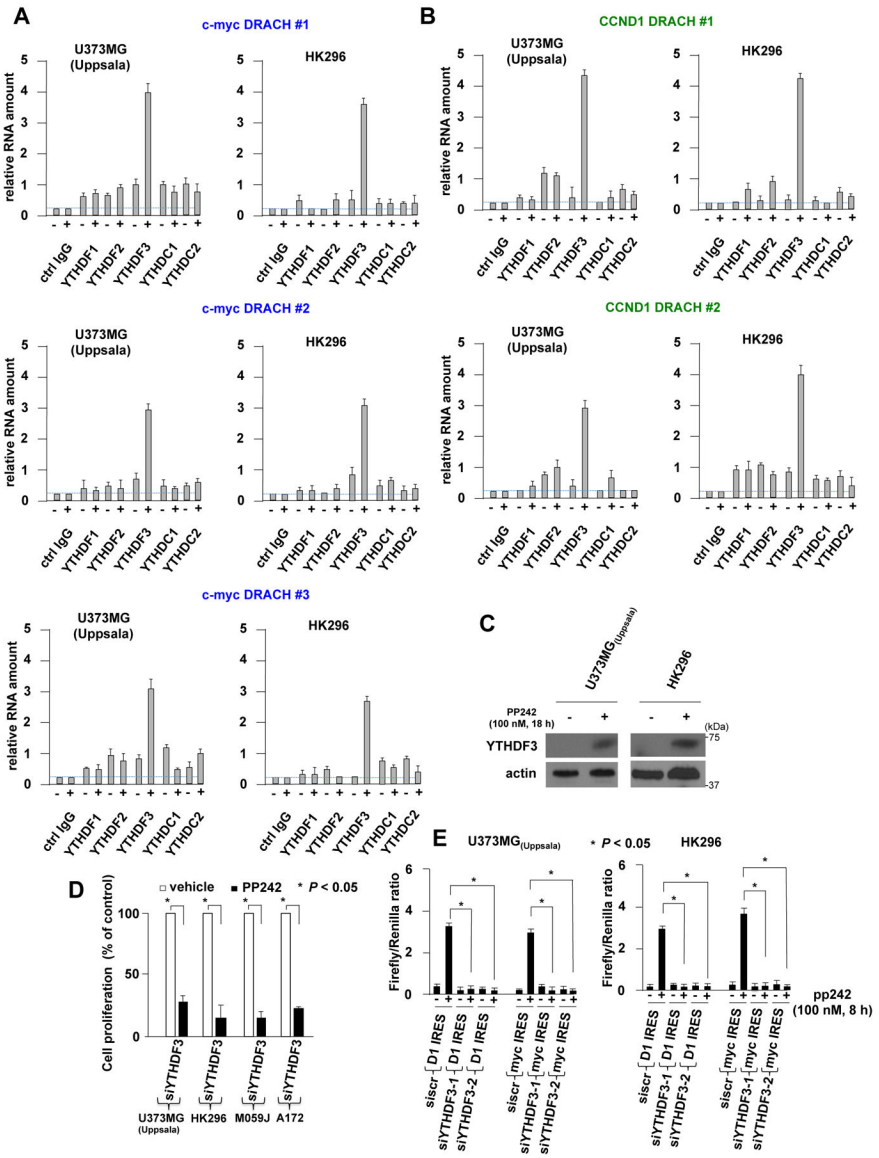

Fig. 6.

YTHDF3 specifically interacts with DRACH RNA motifs in cyclin D1 and c-myc IRESs to regulate IRES activity and mTOR inhibitor sensitivity. **(A)** Screening of YTH domain family proteins binding to the c-myc DRACH RNA motifs (motifs 1–3, see fig. 2A) in $U373MG_{(Uppsala)}$ or HK296 GBM cells in the absence or presence of PP242 as indicated (100 nM, 18 h). The indicated proteins were immunoprecipitated from lysates and bound RNAs were amplified using primers specific for the hairpin sequences. + S.D., n = 4. **(B)** as in **(A)** except binding to the two CCND1 DRACH RNA motifs (motifs 1–2, see fig. 2A) were assessed. **(C)** Induction of YTHDF3 protein expression following PP242 exposure (100 nM, 18 h) in the indicated lines. **(D)** siRNA mediated knockdown of YTHDF3 sensitizes PP242 resistant GBM lines to PP242 (100 nM, 48 h). ATP-release assays were performed (Promega CellTiter-Glo® assay) and cell proliferation determined as a percentage of control vehicle treated cells +S.D.; n = 3. **(E)** siRNA mediated knockdown

of YTHDF3 inhibits PP242 induced IRES activity. U373MG$_{(Uppsala)}$ or HK296 cells were transfected with the indicated non-targeting control (scrambled sequence; shscr) or two individual (siYTHDF3–1 or −2) YTHDF3 targeting siRNAs and IRES activity determined from CCND1 or c-MYC dicistronic mRNA reporters in the absence or presence of PP242 as indicated. Luciferase activity was normalized to the luciferase mRNA level. * *P*-values are shown. Mean + S.D., n = 3.

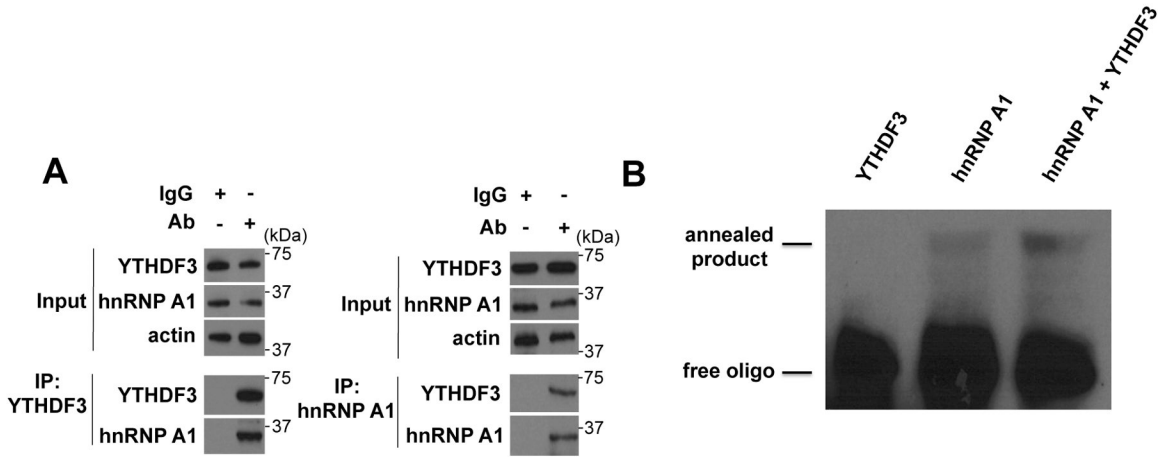

Fig. 7.

hnRNP A1 and YTHDF3 interact and hnRNP A1-induced nucleic acid annealing activity is stimulated by YTHDF3. **(A)** Extracts from U373MG$_{(Uppsala)}$ cells were immunoprecipitated with nonspecific IgG (control) or antibody against YTHDF3 (*left panel*) or hnRNP A1 (*right panel*) and immunoprecipitates immunoblotted for the indicated proteins. Input lysates were probed for the indicated proteins as shown. **(B)** Recombinant YTHDF3 or hnRNP A1 was purified and analyzed for reannealing activity. 1 pmol of each protein was used in the annealing reactions and the migration positions of the indicated species are displayed.